Molecular Catalysis 453 (2018) 93–99

Contents lists available at ScienceDirect

Molecular Catalysis

journal homepage: www.elsevier.com/locate/mcat

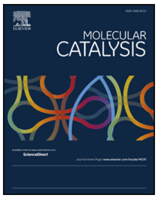

Polyoxoniobates as a superior Lewis base efficiently catalyzed Knoevenagel condensation

Qiaofei Xu, Yanjun Niu, Guan Wang, Yingguang Li, Yuan Zhao, Vikram Singh, Jingyang Niu*, Jingping Wang*

Henan Key Laboratory of Polyoxometalate Chemistry, Institute of Molecule and Crystal Engineering, College of Chemistry and Chemical Engineering, Henan University, Kaifeng, Henan 475004, PR China

ARTICLE INFO

Keywords:
Polyoxoniobates
Base catalysis
Knoevenagel condensation
Natural population analysis

ABSTRACT

The outstanding basicity of negative charged Lindqvist type Polyoxoniobate $K_7HNb_6O_{19}{\cdot}13H_2O$ (Nb_6) have been proved experimentally as well as by theoretical NBO calculations, the results insights high electron density on terminal and bridging oxygen atoms of niobate anion. The most negative Natural Bond Orbital charge (NBO) of oxygen in Nb_6 is −1.001, which is a much more negative value than those reported in other polyoxometalates, that corroborates its high basicity thus likely to be employed as a strong base catalyst. Experimental study suggests that Nb_6 can efficiently catalyze Knoevenagel condensation of various carbonyl compounds with active methylene compounds neglecting the steric and electronic effect of aromatic aldehydes under mild conditions. Kinetic test shows that Knoevenagel condensation of benzaldehyde with ethyl cyanoacetate exhibits second-order kinetics in the presence of Nb_6 and the calculated activation energy is 43.3 kJ mol^{-1}. Meanwhile, a proper mechanism according to the NBO study speculates that the most negative charged terminal oxygens in Nb_6 would be pivotal in this transformation.

1. Introduction

Olefination is one of the most fundamental reactions where the products exert enormous importance on organic synthesis [1]. As a kind of C═C bonds-forming reactions, Knoevenagel condensation reaction is a crucial method to produce olefins using active methylene group reactivity with diverse functional groups via the coupling reaction of carbonyl compounds in the presence of base catalysts along with the loss of molecular H_2O in the suitable reaction conditions. This reaction is of prime importance in many significant areas of research like synthesis of various reaction intermediates, products for perfumes, calcium antagonists, polymers and in pharmaceutical industries [2,3]. Traditionally, the solid bases [4,5], Lewis acids [6,7], and organometallic compounds [8,9] were applied as catalysts in the process, while they are lack in their efficiency, robustness, and recyclability [10]. Therefore, considerable research efforts have been focused on this reaction by using various catalysts, such as metal-organic frameworks [11,12], ionic liquid [13], molecular complexes [14] and etc.

Polyoxometalates (POMs) as a class of anionic metal-oxide clusters mainly obtained by the condensation reaction of corresponding oxysalts or metallic oxides. Structurally, POMs are constructed by the corner-, edge-, or face-shared fashion of metal oxide polyhedral (MO_x: M = W^{VI}, Mo^{VI}, V^V, Nb^V, Ta^V, etc., and x = 4–7), thus leading to provides novel building units for the assembly of larger systems [15–17]. Moreover, POMs have exhibited remarkable performance in many fields, such as fluorescence [18], magnetism [19], drugs [20], electrochemistry [21], and especially in catalysis [22–25]. To date, many applications involving POMs incorporated V^V, Mo^{VI}, and W^{VI} were investigated in various types of catalytic reactions including acid catalysis [26–29], oxidation catalysis [30–34], photocatalysis [35–37] and electro-catalysis [38–41] mainly due to their redox tunable behavior, low pH stability, high thermal resistivity and photoelectric behaviors [42]. However, there were few reports which deals on the basic catalytic performance of POMs [43–45]. In general, it is well known that POMs possess strong acidity thus the weak basicity of their conjugate base restricts to support them as outstanding base catalysts. Actually, outstanding works on Knoevenagel condensation reaction have shown that polyoxotungstates (POTs) exhibited fascinating performance in this process. Mizuno et al. firstly reported the superior catalytic reactivity of alkaline disilicoicosatungstates $[H(\gamma\text{-}SiW_{10}O_{32})_2(\mu\text{-}O)_4]^{7-}$ than the acidic di $[\{\gamma\text{-}SiW_{10}O_{32}(H_2O)_2\}_2(\mu\text{-}O)_2]^{4-}$ for Knoevenagel condensation reaction in the similar reaction conditions[46]. Subsequently, Mizuno and coworkers revealed that $[\gamma\text{-}H_2GeW_{10}O_{36}]^{6-}$can act as an efficient base catalyst for Knoevenagel condensation [47]. Later, Song et al. also

---

* Corresponding authors.
E-mail addresses: jyniu@henu.edu.cn (J. Niu), jpwang@henu.edu.cn (J. Wang).

https://doi.org/10.1016/j.mcat.2018.05.002
Received 9 March 2018; Received in revised form 23 April 2018; Accepted 3 May 2018

explored highly charged tri-lacunary polyanoins i.e. $Na_8H[A\text{-}PW_9O_{34}]$ and $Na_8H[B\text{-}PW_9O_{34}]$ as catalysts for cyanosilylation and Knoevenagel condensation reactions, respectively [48]. Beside these, it is well documented that POTs supported on graphene oxide [49] and LDH (Layered double hydroxides) [50] also show excellent performance as the catalyst for Knoevenagel condensation. However, polyoxoniobates (PONs) as an important subclass of POMs have been investigated relatively in synthetic chemistry but it is seldom explored in catalysis. Hence, it is significant to open a new way for their applications in catalytic direction.

According to literatures, more electronegative oxygen atoms provide higher basicity in POMs, which could be approximately deduced by comparison of their "charge-density" as: Charge-density (charge/atom) = (anionic charge of the POM)/(number of non-hydrogen atoms of the POM) [51,52]. From the charge-density of conventional PONs and POTs: $[Nb_6O_{19}]^{8-}$ (0.32), $[Ti_2Nb_8O_{28}]^{8-}$ (0.21), $[Nb_{10}O_{28}]^{6-}$ (0.16), $[SiNb_{12}O_{40}]^{16-}$ (0.30), $[(PO_2)_3PNb_9O_{34}]^{15-}$ (0.28), $[H_2Si_4Nb_{16}O_{56}]^{14-}$ (0.18), $[W_6O_{19}]^{2-}$ (0.08), $[SiW_{12}O_{40}]^{4-}$ (0.075), $[SiW_{11}O_{39}]^{8-}$ (0.16), $[PW_9O_{34}]^{9-}$ (0.20), it is obvious that PONs possess higher charge-density than POTs. However, to date, only two works were reported on PONs catalyzed Knoevenagel condensation reaction: Tsukuda et al. reported that the $(TMA)_6[Nb_{10}O_{28}]$ can be regarded as an efficient base catalyst for this process [51]; Wang et al. discovered $Na_{16}[SiNb_{12}O_{40}]$ as a base catalyst for catalyzing CO_2 cycloaddition and Knoevenagel condensation [53]. Notably, $[Nb_6O_{19}]^{8-}$ shows the highest charge-density in these compounds including $[SiNb_{12}O_{40}]^{16-}$ and $[Nb_{10}O_{28}]^{6-}$, which suggests the wonderful basicity of $[Nb_6O_{19}]^{8-}$ which facilitates them as the best candidates for Knoevenagel condensation reaction. In addition, $K_7HNb_6O_{19}\cdot 13H_2O$ (Nb_6) is easily prepared with high yield, which may provide the potential catalytic use in its application.

Herein, we employed Nb_6 as a base catalyst in Knoevenagel condensation reaction, which exhibited excellent catalytic performance for the condensation of various aldehydes and ketones at mild reaction conditions. Furthermore, theoretical calculation for the basicity of $[Nb_6O_{19}]^{8-}$ and the comparison with other POMs (including PONs and POTs) was also executed by density functional theory (DFT). On the basis of DFT calculations results, it can be concluded that the most negative NBO (Natural Bond Orbital) charge in $[Nb_6O_{19}]^{8-}$ is −1.001 which is much higher than the NBO charge of WO_4^{2-} (the index of strong basicity which is −0.934 [53]) and other POMs. Moreover, the terminal oxygens possess more negative charge than bridging oxygens with in $[Nb_6O_{19}]^{8-}$, which can be regarded as the basic catalytic sites in the catalytic reaction.

2. Results and discussion

2.1. Basicity study

According to the literature, the basic active sites are located at the oxygen atom on the surface of POMs, and the higher negatively charged polyanions may possess stronger basicity [51]. Herein, the basicity of Nb_6 was investigated by NBO and compared with other three polyanions ($W_6O_{19}^{2-}$: W_6; $Nb_{10}O_{28}^{6-}$: Nb_{10}; $SiW_{12}O_{40}^{4-}$: SiW_{12}). As shown in Fig. 1a, the oxygen atoms charge in Nb_6 by NBO analysis are divided into five species corresponding to the values −0.809, −0.859, −0.869, −0.975, −1.001, where red rhombuses and blue circles represented the charge of terminal oxygens and bridging oxygens in Nb_6, respectively. Obviously, the terminal oxygens possess more negative charge than bridging oxygens with in Nb_6, which is different from Nb_{10} but the same to $SiNb_{12}O_{40}^{16-}$ ($SiNb_{12}$) [51,53]. Additionally, there is the comparison of the most negative charge among Nb_6 and three above polyanions in Fig. 1b, where the data spots presented the most negative charge in these compounds. The results showed that the most negative charge of Nb_6 is much higher than those of $W_6O_{19}^{2-}$ (−0.719), $Nb_{10}O_{28}^{6-}$ (−0.884), SiW_{12}^{4-} (−0.750). It must be mentioned that the NBO charges of oxygen atoms in Nb_6 are even more negative than the one (−0.934) in WO_4^{2-}, which imply that the superior basicity of Nb_6 is likely to be used as the base catalyst.

2.2. Catalysis

Considering the splendid basicity of Nb_6 has, it was employed as a base catalyst for Knoevenagel condensation reaction. Initially, the condensation reaction of benzaldehyde with ethyl cyanoacetate was carried out with different catalysts. The results of parallel experiments have been presented in Table 1, which have shown that there was little reactivity of this transformation in the absence of catalyst (entry 1). However, there was a great improvement in yield of product with NaOH loading in this system (entry 2), which has implied that the process benefited from basicity. Therefore, the lacunary POTs (entries 5, 7,11, 12) are more active than the plenary ones (entries 8, 9, 10, 13). In addition, precursors of Nb_6 (Nb_2O_5, $Nb_2O_5\cdot xH_2O$) have no obvious activity for the reaction. Strikingly, Nb_6 has exhibited the best catalytic performance for the reaction at the same conditions, which is in good consistent with its splendid basicity.

2.3. Influence of different factors on the process

To our best knowledge, reaction temperature, dosage of catalyst, raw ratio and solvents all play critical roles in this process, which were investigated in detail via the condensation reaction of benzaldehyde with ethyl cyanoacetate as the model reaction catalyzed by Nb_6 in various conditions. As shown in Fig. 2a, when 0.1 mol% catalyst was employed, 91% of yield for the reaction could be obtained. Moreover, the increase of yield would continue by the addition of the mass loading. Obviously, more catalytic dosage would improve the reaction rate. As to the effect of temperature, the results of condensation of benzaldehyde with ethyl cyanoacetate were studied at different temperatures shown in Fig. 2b. From 25 °C to 40 °C, there is a remarkable improvement in the yield of product. With the increase of temperature going on from 40 °C to 60 °C, there is also an enhancement of product and when the temperature comes to 60 °C, the highest yield of product was obtained corresponding to the yield of 98%. Considering the effect of raw ratio, the results of 0.6: 1, 0.8:1, 1:1 and 1.2:1 (donor: acceptor) have been presented in Fig. 2c, which showed that any ratio could be quicker to reach the limitation of the reaction than expected 1:1. Given that solvents also have an effect on this reaction, consequently, several contrast experiments were performed in various solvents. As the results shown in Fig. 2d, the catalyst in C_2H_5OH has the best performance for the process where an excellent yield of 98% has been obtained. Meanwhile, Nb_6 also exhibited good yield although the reaction took place in various solvents, which suggested that Nb_6 could be regarded as a wonderful catalyst for processing the Knoevenagel condensation of benzaldehyde with ethyl cyanoacetate.

2.4. Kinetic study

In order to obtain the kinetic parameters of the reaction, several catalytic experiments were performed by mixing catalyst, benzaldehyde and ethyl cyanoacetate in ethanol at different times and temperatures. Fig. 3a–d are the plots obtained for the yield of product and $C/[C_0(C_0 - C)]$ as the function of reaction time, where C is the corresponding concentration of benzaldehyde transformed to product at time t and initial concentration of benzaldehyde is C_0. As indicated by stars in Fig. 3a–d, they fall into the quasi-linear plot of reaction time and $C/[C_0(C_0 - C)]$, which reveals that the reaction catalyzed by Nb_6 exhibits second-order kinetics for the Knoevenagel condensation. The different rate constants (k_1, k_2, k_3, k_4) were determined at corresponding temperature (25 °C, 40 °C, 50 °C, 60 °C, respectively) according to Eqs. (1) and (2), which have been calculated as follows: k_1 = 0.03551 (mol/L)$^{-1}$(min)$^{-1}$, k_2 = 0.08954 (mol/L)$^{-1}$(min)$^{-1}$ k_3 = 0.14981 (mol/

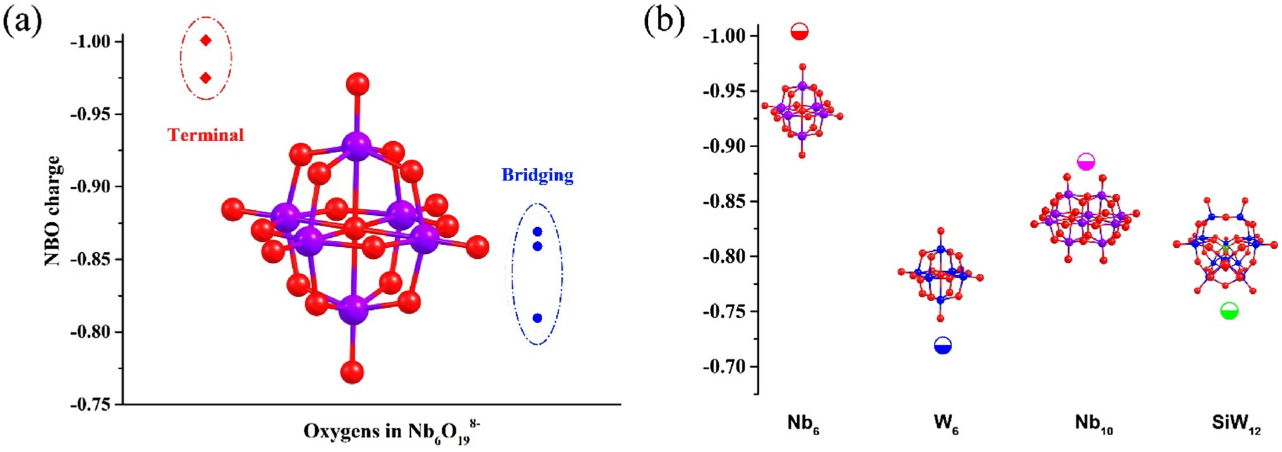

Fig. 1. (a) The NBO charges of oxygens in Nb_6; (b) the comparison of Nb_6, W_6, Nb_{10}, SiW_{12}. (Nb: purple, W: blue, Si: green, O: red.).

Table 1
Knoevenagel condensation of benzaldehyde with ethyl cyanoacetate was performed with various catalysts.

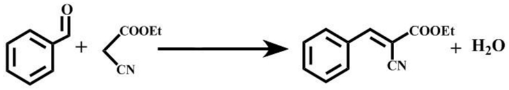

Entry	Catalyst	Yield[b]/%
1[a]	–	4.4
2	Nb_2O_5	6.3
3	$Nb_2O_5{\cdot}xH_2O$	10
4	NaOH	93
5	K_8SiW_{10}	84
6	$K_7HNb_6O_{19}$	98
7	$Na_8HPW_9O_{34}$	86
8	$H_3PW_{12}O_{40}$	11
9	$K_3AsW_{12}O_{40}$	11
10	$H_6P_2W_{18}O_{62}$	14
11	$Na_{12}P_2W_{15}O_{56}$	68
12	$Na_6P_2W_{12}O_{42}$	84
13	$K_5BW_{12}O_{40}$	9

[a] Reaction conditions: catalyst 5 μmol, benzaldehyde 1 mmol, ethyl cyanoacetate 1 mmol, ethanol 1 mL, temperature 60 °C, reaction time 2 h.

[b] GC yields for target product ethyl (E)-acyanocinnamate were based on methylbenzene as internal standard. All of the products were identified by GC–MS spectra and GC spectra.

$L)^{-1}(min)^{-1}$ $k_4 = 0.21875\ (mol/L)^{-1}(min)^{-1}$. Moreover, the calculated activation energy ($Ea = 43.3\ kJ\ mol^{-1}$) of the Knoevenagel condensation of benzaldehyde with ethyl cyanoacetate was obtained according to the Arrhenius equation (Eqs. (3) and (4)), which was shown in Fig. 3e and f detailed.

$$dC/dt = k\ (C_0 - C)^2 \tag{1}$$

$$C/[C_0\ (C_0 - C)] = kt \tag{2}$$

$$k = A\exp\ (-Ea/(RT)) \tag{3}$$

$$\ln k = \ln A - Ea/RT \tag{4}$$

2.5. Scope of substrate

Encouraged by the aforementioned results, Knoevenagel condensation of various aldehydes and ketones with ethyl cyanoacetate and malononitrile catalyzed by Nb_6 have been investigated in C_2H_5OH. As can be seen from Tables 2 and 3, various substrates including aldehydes and ketones were used to investigate the applicability of Nb_6, whose results identified that Nb_6 have exhibited remarkable catalysis for

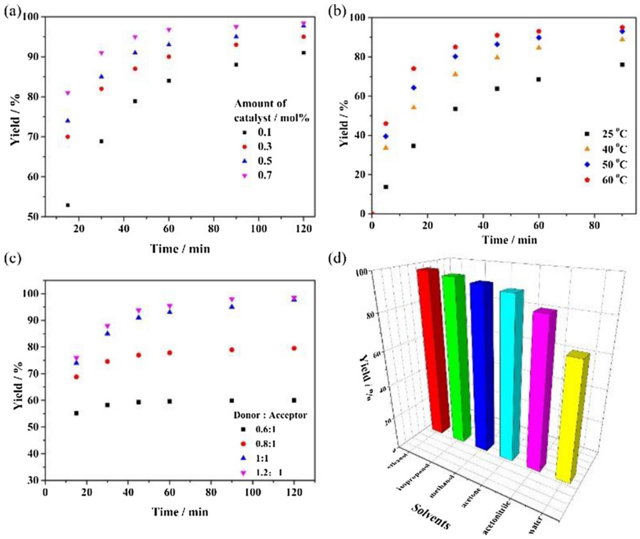

Fig. 2. (a) The polts of amout of catalyst versus time; (b) the polts of temperature versus time; (c) the polts of raw ratio versus time; (d) the histogram of yield in different solvents GC yield for target product ethyl (E)-acyanocinnamate. All of the products were identified by GC–MS spectra and ^1H NMR spectra.

Knoevenagel condensation of various functional groups (electron-donating and electron withdraw) substituted benzaldehydes with ethyl cyanoacetate (Table 2, entry 1–14) or malononitrile (Table 3, entry 1–13). Specifically, yield of ≥95% were achieved for the condensation of substituted benzaldehydes and hexahydrobenzaldehyde with ethyl cyanoacetate at the ortho-, meta- and para-positions, respectively (Table 2, entry 1–12) and completely neglected the steric effect and electronic effect, which exhibits outstanding universality for substituted benzaldehydes. Nevertheless, the condensation of ketone with ethyl cyanoacetate only obtained the yield of 38% and 48% (Table 2, entry 13–14).

Malononitrile as similar nucleophile shows stronger reactivity than ethyl cyanoacetate in the present of Nb_6, leading to the yield of 99% for Knoevenagel condensation of benzaldehyde with malononitrile at room temperature after 45 min. Moreover, this successful approach towards Knoevenagel condensation with malononitrile showed that the wonderful catalysis could be performed with other substituted benzaldehydes, hexahydrobenzaldehyde and ketones after prolonging the reaction time (Table 3, entry 13–14). Meanwhile, on the basis of these results, we can conclude that aldehydes are more active than ketones in the transformation.

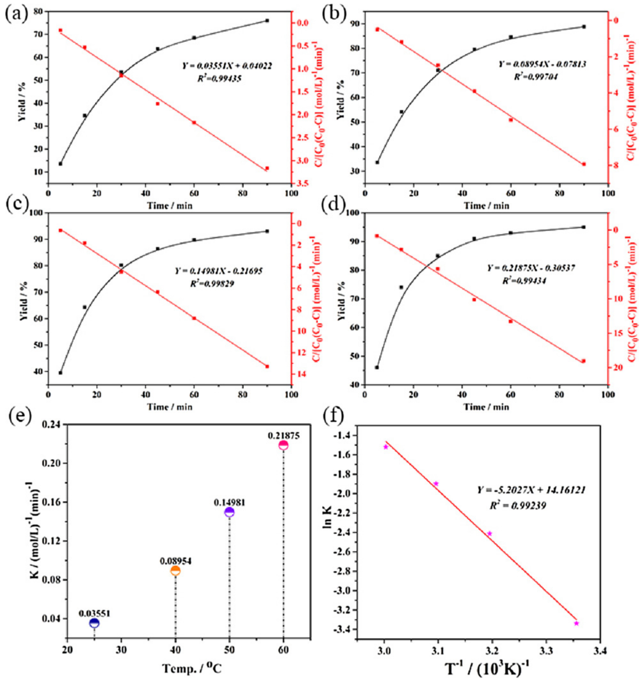

Fig. 3. (a)–(d): Kinetic profiles of the Knoevenagel condensation of benzaldehyhde with ethyl cyanoacetate catalyzed by Nb_6 in different temperatures: (a) 25 °C; (b) 40 °C; (c) 50 °C; (d) 60 °C. (e): the different *k* at corresponding temperature; (f): the quasi-linear plot of lnk and T^{-1}.

Table 2
Knoevenagel condensation of various substrateswith ethyl cyanoacetate inthe presence of Nb_6.

Entry	Acceptor		Product		Yield[b]/%
1[a]	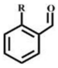	R_1 = Cl	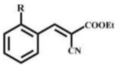	R_1 = Cl	99
2		R_2 = NO_2		R_2 = NO_2	99
3		R_3 = CH_3O		R_3 = CH_3O	99
4	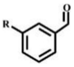	R_1 = Cl	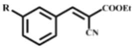	R_1 = Cl	99
5		R_2 = NO_2		R_2 = NO_2	99
6	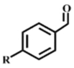	R_1 = F	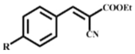	R_1 = F	98
7		R_2 = Cl		R_2 = Cl	99
8		R_3 = Br		R_3 = Br	99
9		R_4 = CH_3		R_4 = CH_3	98
10		R_5 = CH_3O		R_5 = CH_3O	97
11		R_6 = NO_2		R_6 = NO_2	98
12	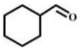		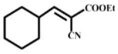		98
13			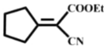		48
14	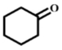		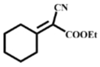		38

[a] Reaction conditions: catalyst 5 μmol, benzaldehyde 1 mmol, ethyl cyanoacetate 1 mmol, ethanol 1 mL, temperature 60 °C, reaction time 2 h.
[b] GC yield for target product.

2.6. Comparison of different catalysts for Knoevenagel condensation reaction

In addition, a comparison of the efficiency of Nb_6 with previously reported catalysts for the Knoevenagel condensation was presented in Table 4. The results have shown that although many previously reported catalysts displayed good catalysis for Knoevenagel condensation, most of the reported catalytic systems need higher temperature and longer time to obtain excellent catalytic performance, where Nb_6 has a better economic substitute as to save time and resources. Ideally, 1:1 stoichiometry should be the best choice than any proportion. Therefore, on the basis of these findings, it has been confirmed that Nb_6 as a robust basic catalyst has presented high efficiency for catalyzing Knoevenagel condensation.

Table 3
Knoevenagel condensation of various substrates with malononitrile in the presence of Nb_6.

Entry	Acceptor		Product		Yield[c]/%
1[a]	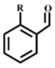	R_1 = Cl	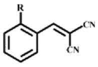	R_1 = Cl	100
2		R_2 = NO_2		R_2 = NO_2	97
3		R_4 = H		R_4 = H	99
4	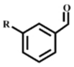	R_1 = Cl	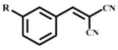	R_1 = Cl	100
5		R_2 = NO_2		R_2 = NO_2	100
6	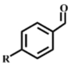	R_1 = F	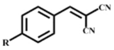	R_1 = F	96
7		R_2 = Cl		R_2 = Cl	100
8		R_3 = Br		R_3 = Br	100
9		R_4 = CH_3		R_4 = CH_3	98
10		R_6 = NO_2		R_6 = NO_2	99
11	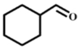		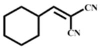		95
12[b]	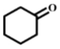		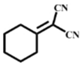		99
13	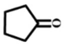		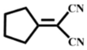		88

[a] Reaction conditions: catalyst 5 μmol, benzaldehyde 1 mmol, ethyl cyanoacetate 1 mmol, ethanol 1 mL, temperature 25 °C, reaction time 45 min.
[b] Reaction conditions: catalyst 5 μmol, benzaldehyde 1 mmol, malononitrile 1 mmol, ethanol 1 mL, temperature 25 °C, reaction time 3 h.
[c] GC yield for target product.

Table 4
The comparison of the efficiency of Nb_6 with previously reported catalysts for the Knoevenagel condensation.

Catalyst	Donor: Acceptor	Temp./°C	Time/h	Yield/%	Ref.
Nb_6	1:1	60	2	98	This work
Mg_3Al-PW_{12}	1.5:1	60	6	> 99	[50]
$Na_{16}SiNb_{12}O_{40}$	1:1	70	2	97	[53]
$(TMA)_6[Nb_{10}O_{28}]\cdot 6H_2O$	1:1	70	24	88	[51]
[Nmm-PDO][OAc]	1:1	rt	6	96	[10]
$Na_8H[A$-$PW_9O_{34}]$	1.5:1	rt	6	80	[48]
ED-MIL-101	1:1	80	19	97	[54]
ED-MIL-101(D)	1:1	80	7	97	
APS-MIL-101	1:1	80	19	96	
UPC-30	1:1	rt	5	94	[55]
aminopropyl-functionalized MCM	1:1	82	36	94	[56]
organic-inorganic hybrid silica material	1.1:1	130	2	> 99	[57]
DMAN/SiO2	1:1.14	60	6	> 99	[58]

2.7. Recyclability

The reusability of catalyst was evaluated by using Nb_6 (20 mg) to catalyze Knoevenagel condensation of benzaldehyde (1 mmol) with ethyl cyanoacetate (1 mmol) at 60 °C in 2 h.

Subsequently, insoluble Nb_6 can be recovered easily from the mixture of solvent/substrates/catalyst by filtration at the end of every cycle. Besides, traces of Nb in the filtrate have not been detected by inductively coupled plasma spectrometer(ICP), which also shows it exhibited as a good heterogeneous catalyst. Organic compounds were removed completely by solvent evaporation at 60 °C leading to the catalyst left in the tube then after washed three times by alcohol. The infrared spectrum of Nb_6 after every cycle was used to analyze catalyst composition, followed by a duplicate test mainly proceeded with the

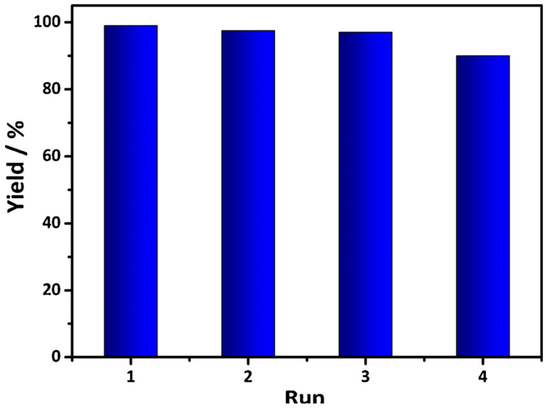

Fig. 4. The histogram of yield of product for reused catalyst.

unchanged catalyst. The results for recyclability of Nb_6 have been shown in Table S3, which indicated that there is a yield of 90% even at fourth run. Unfortunately, the infrared spectrum of reused catalyst in Fig. S2 revealed that Nb_6 has changed after the third run, which is corresponding to the results in Fig. 4 and the changes for the traces of Nb after the third catalytic recycle (Nb, 54.63%).

2.8. Mechanism study

Although there is no clear reaction pathway, a proposed plausible mechanism for Knoevenagel condensation of aldehydes with active methylene compounds has been presented in Scheme 1 [13]. Terminal oxygens in Nb_6 exhibit more negative NBO charges corresponding to the higher basicity, hence, we speculated that the reactions are likely proceeded by the general base mechanism [44]. As Scheme 1 shows, the O atom in Nb=O is considered to carry off one acidic proton from the active methylene compounds to produce the corresponding carbanion which is regarded as a nucleophile used to attack C atom in aldehyde group to generate new C—C bond. The alkoxide ions would capture the proton from the protonated catalyst leading to the β-hydroxyl compounds and regenerative catalyst. Finally, the product will be obtained in dependence on the dehydration of β-hydroxyl compounds.

3. Materials and methods

3.1. Materials

All of the reagents used were of analytical grade and obtained from commercial sources without further purification. $K_7HNb_6O_{19}{\cdot}13H_2O$ was prepared using literature methods and characterized by IR spectroscopy and X-ray powder diffraction [59]. All of the reactants were purchased from J&K Chemical.

3.2. Catalyst synthesis

$K_7HNb_6O_{19}{\cdot}13H_2O$ was prepared according to the literature and characterized by IR spectrum (Fig. S1) and X-ray powder diffraction. In a typical procedure, commercial Nb_2O_5 (13.3 g) was added to the melt KOH in a nickel crucible. The melt was cooled down to room temperature and added 100 mL deionized water in the nickel crucible after heating 30 min. Followed by filtration of the above mixture and then putting the solution in refrigerator at 0 °C after 12 h will lead to the solid (some crystals) which can be obtained via filtration. Finally, the solid was washed with 1:1 (V/V) ethanol-water and dried in vacuo resulting solid was denoted as Nb_6. Elemental analysis (%) calcd for Nb_6: Nb, 40.70. Found: Nb, 39.57. The polyanion of one above crystal in obtained solid has been identified as Lindqvist Nb_6 by X-ray single crystal diffraction, whose polyhedron view has been shown in Fig. S3a. Furthermore, the XRD pattern in Fig. S3b of the obtained solid is in coincidence with the simulated XRPD patterns of Nb_6 implying that the sample for catalysis is pure.

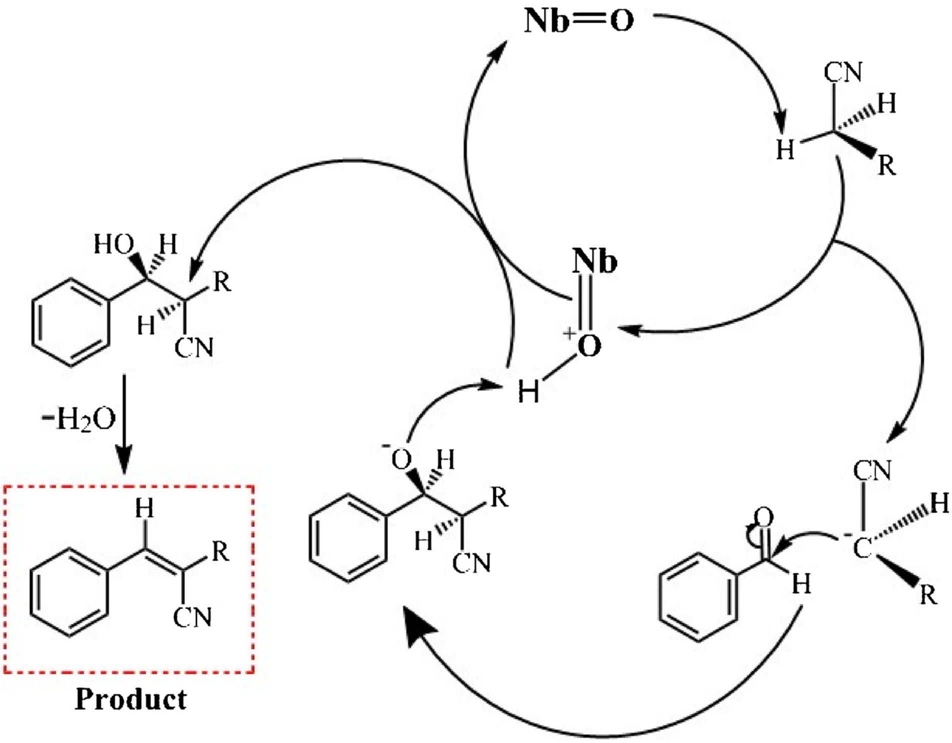

Scheme 1. Proposed mechanism for Knoevenagel condensation of aldehydes with active methylene compounds.

3.3. General procedure for the Knoevenagel condensation

The aldehydes (1 mmol), active methylene compounds (1 mmol), catalyst (0.5 mol%) and solvent (1 mL) were added into a tube at room temperature. The reaction mixture was stirred and heated at the prescribed conditions on the parallel reactor. The product carried on qualitative detection by GC–MS and the yield was monitored by GC. Followed by using ethanol to wash the catalyst 3 times and then dried in vacuo at 60 °C.

3.4. Characterization

IR spectra were recorded on a Bruker VERTEX 70 IR spectrometer (using KBr pellets) in the range of 4000–400 cm^{-1}. X-ray powder diffraction (XRPD) data were recorded on a Bruker AXS D8 Advance diffractometer (Bruker, Karlsruhe, Germany) with Cu Kα radiation in the angular range $2\theta = 5°–45°$ at 293 K.

3.5. Calculations

The structure of four POMs are optimized by using Becke's three-parameter nonlocal-exchange functional with the nonlocal correlation functional of Lee-Yang-Parr method [60,61]. The 6-31G(d) basis set is used for atoms of O and Si. The heavy atoms of Nb and W are described with LANL2DZ basis set, which obtained from the EMSL data base [62,63]. The harmonic vibrational frequencies are also performed at the same level to affirm the stationary points as minima. The Cartesian coordination of compounds and their lowest five frequencies are listed in Tables S1–S5. The bond lengths agree well with the corresponding experimental values error within 5%, indicating that the calculated geometries are reliable. On basis of the optimized structures, the localized charges of the atoms are acquired by utilizing Natural population analysis (NPA), which is shown in Fig. 1. Herein the B3LYP method has been also used. In order to obtain more reliable results, the basis set of 6-31 + G(d) is utilized for O and Si, and LANL2TZ(f) is used for depicting Nb and W atoms. It can be seen that NPA charges of Nb_6. The whole calculations are carried out by using Gaussian 09 software.

4. Conclusion

In this work, we reported that Nb_6 can be used as an efficient Lewis base catalyst for Knoevenagel condensation. Theoretical calculation shows that Nb_6 could be an important candidate as the strong base catalyst due to its highly negative charge (−1.001) which is higher than the index of high basicity (−0.934, the high charge density calculated by density functional theory). As expected, it is in a good agreement commensurate with the theory and experimental results: Knoevenagel condensation reactions were catalyzed by Nb_6 which has presented ≥95% of products, devoid of any influence of the steric and electronic effect of aromatic aldehyde. Kinetic study shows that the Knoevenagel condensation exhibits second-order kinetics in the presence of Nb_6. A proper mechanism was presented to speculate the reaction process based on the NBO analysis. Moreover, high efficiency, recyclability and easy production of Nb_6 provide more possibility for its future application.

Acknowledgments

This work was supported by the National Natural Science Foundation of China (Grants 21371048, 21671056 and21603057), the Natural Science Foundation of Henan Province (Grant134300510035), Special Program for Applied Research on Super Computation of the NSFC-Guangdong Joint Fund (the second phase) under Grant No. U1501501.

Appendix A. Supplementary data

Supplementary data associated with this article can be found, in the online version, at http://dx.doi.org/10.1016/j.mcat.2018.05.002.

References

[1] J. Li, G. Liu, L. Shi, Q. Xing, F. Li, Cobalt modified N-doped carbon nanotubes for catalytic C–C bond formation *via* dehydrogenative coupling of benzyl alcohols and DMSO, Green Chem. 19 (2017) 5782–5788.
[2] E.M. Schneider, M. Zeltner, N. Kranzlin, R.N. Grass, W.J. Stark, Base-free Knoevenagel condensation catalyzed by copper metal surfaces, Chem. Commun. 51 (2015) 10695–10698.
[3] C.I. Ezugwu, B. Mousavi, M.A. Asraf, Z. Luo, F. Verpoort, Post-synthetic modified MOF for Sonogashira cross-coupling and Knoevenagel condensation reactions, J. Catal. 344 (2016) 445–454.
[4] Y.X. Wang, L.J. Wang, C.P. Liu, R.H. Wang, Benzimidazole-containing porous organic polymers as highly active heterogeneous solid-base catalysts, ChemCatChem 7 (2015) 1559–1565.
[5] S. Fujita, A. Katagiri, H. Watanabe, S. Asano, H. Yoshida, M. Arai, Preparation of nitrogen-doped carbon from polyacrylonitrile and its application as a solid-base catalyst, ChemCatChem 7 (2015) 2965–2970.
[6] A. Dandia, V. Parewa, A.K. Jain, K.S. Rathore, Step-economic, efficient, ZnS nanoparticle-catalyzed synthesis of spirooxindole derivatives in aqueous medium via Knoevenagel condensation followed by Michael addition, Green Chem. 13 (2011) 2135–2145.
[7] B.K. Parvanak, P. Ghasemi, Synthesis and application of a novel strong and stable supported ionic liquid catalyst with both Lewis and Brønsted acid sites, Catal. Commun. 37 (2013) 50–54.
[8] D. Fildes, V. Caignaert, D. Villemin, P.A. Jaffres, Potassium exchanged zirconium hydrogen phosphate $Zr(O_3POK)_2$: a heterogeneous basic catalyst for Knoevenagel reaction without solvent, Green Chem. 3 (2001) 52–56.
[9] K. Yamashita, T. Tanaka, M. Hayashi, Use of isopropyl alcohol as a solvent in Ti(O-*i*-Pr)$_4$-catalyzed Knöevenagel reactions, Tetrahedron 61 (2005) 7981–7985.
[10] H. Xu, L. Pan, X. Fang, B. Liu, W. Zhang, M. Lu, Y. Xu, T. Ding, H. Chang, Knoevenagel condensation catalyzed by novel Nmm-based ionic liquids in water, Tetrahedron Lett. 58 (2017) 2360–2365.
[11] S.F. Amarante, M.A. Freire, D.T.S.L. Mendes, L.S. Freitas, A.L.D. Ramos, Evaluation of basic sites of ZIFs metal organic frameworks in the Knoevenagel condensation reaction, Appl. Catal. Gen. 548 (2017) 47–51.
[12] J. Juan-Alcañiz, E.V. Ramos-Fernandez, U. Lafont, J. Gascon, F. Kapteijn, Building MOF bottles around phosphotungstic acid ships: one-pot synthesis of bi-functional polyoxometalate-MIL-101 catalysts, J. Catal. 269 (2010) 229–241.
[13] D. Elhamifar, S. Kazempoor, B. Karimi, Amine-functionalized ionic liquid-based mesoporous organosilica as a highly efficient nanocatalyst for the Knoevenagel condensation, Catal. Sci. Technol. 6 (2016) 4318–4326.
[14] S.K. Panja, N. Dwivedi, S. Saha, First report of the application of simple molecular complexes as organo-catalysts for Knoevenagel condensation, RSC Adv. 5 (2015) 65526–65531.
[15] L. Yang, L. Li, J. Guo, Q. Liu, P. Ma, J. Niu, J. Wang, A nanosized gly-decorated praseodymium-stabilized selenotungstate cluster: synthesis, structure, and oxidation catalysis, Chem. – Asian J. 12 (2017) 2441–2446.
[16] P. Ma, F. Hu, Y. Huo, D. Zhang, C. Zhang, J. Niu, J. Wang, Magnetoluminescent bifunctional dysprosium-based phosphotungstates with synthesis and correlations between structures and properties, Cryst. Growth Des. 17 (2017) 1947–1956.
[17] S. Hayashi, S. Yamazoe, K. Koyasu, T. Tsukuda, Lewis base catalytic properties of $[Nb_{10}O_{28}]^{6-}$ for CO_2 fixation to epoxide: kinetic and theoretical studies, Chem. – Asian J. 12 (2017) 1635–1640.
[18] J. Wang, Y. Liang, P. Ma, D. Zhang, J. Niu, J. Wang, Ligand-controlled formation of covalently modified antimoniomolybdates and their photochromic properties, CrystEngComm 19 (2017) 207–213.
[19] P. Ma, F. Hu, R. Wan, Y. Huo, D. Zhang, J. Niu, J. Wang, Magnetic double-tartaric bridging mono-lanthanide substituted phosphotungstates with photochromic and switchable luminescence properties, J. Mater. Chem. C 4 (2016) 5424–5433.
[20] A. Banerjee, B.S. Bassil, G.V. Röschenthaler, U. Kortz, Diphosphates and diphosphonates in polyoxometalate chemistry, Chem. Soc. Rev. 41 (2012) 7590–7604.
[21] Y. Huo, Z. Huo, P. Ma, J. Wang, J. Niu, Polyoxotungstate incorporating organotriphosphonate ligands: synthesis, characterization, and catalytic for alkene epoxidation, Inorg. Chem. 54 (2015) 406–408.
[22] I.V. Kozhevnikov, Catalysis by heteropoly acids and multicomponent polyoxometalates in liquid-phase reactions, Chem. Rev. 98 (1998) 171–198.
[23] J.C.S. Soares, A.H.A. Gonçalves, F.M.Z. Zotin, L.R.R. de Araújo, A.B. Gaspar, Cyclohexene to adipic acid synthesis using heterogeneous polyoxometalate catalysts, Mol. Catal. (2018) in press.
[24] N. Mizuno, Modern Heterogeneous Oxidation Catalysis: Design, Reactions and Characterization, John Wiley & Sons, 2009.
[25] M.G. Clerici, O.A. Kholdeeva, Liquid Phase Oxidation via Heterogeneous Catalysis: Organic Synthesis and Industrial Applications, John Wiley & Sons, 2013.
[26] J. Kaur, K. Griffin, B. Harrison, I.V. Kozhevnikov, Friedel–crafts acylation catalysed by heteropoly acids, J. Catal. 208 (2002) 448–455.
[27] J. Li, D. Li, J. Xie, Y. Liu, Z. Guo, Q. Wang, Y. Lyu, Y. Zhou, J. Wang, Pyrazinium polyoxometalate tetrakaidecahedron-like crystals esterify oleic acid with equimolar methanol at room temperature, J. Catal. 339 (2016) 123–134.
[28] K.V. Avramidou, F. Zaccheria, S.A. Karakoulia, K.S. Triantafyllidis, N. Ravasio,

Esterification of free fatty acids using acidic metal oxides and supported polyoxometalate (POM) catalysts, Mol. Catal. 439 (2017) 60–71.

[29] Y. Liu, L. Xu, B. Xu, Z. Li, L. Jia, W. Guo, Toluene alkylation with 1-octene over supported heteropoly acids on MCM-41 catalysts, J. Mol. Catal. Chem. 297 (2009) 86–92.

[30] G. Trautwein, B.E. Bakkali, J. Alcañiz-Monge, B. Artetxe, S. Reinoso, J.M. Gutiérrez-Zorrilla, Dimeric assemblies of lanthanide-stabilised dilacunary Keggin tungstogermanates: a new class of catalysts for the selective oxidation of aniline, J. Catal. 331 (2015) 110–117.

[31] H. Yang, B. Jiang, Y. Sun, X. Tantai, X. Xiao, J. Wang, L. Zhang, Construction of polyoxometallate-based organic-inorganic hybrid nanowires for efficient oxidative desulfurization, Mol. Catal. 448 (2018) 38–45.

[32] M. Zhao, X.W. Zhang, C.D. Wu, Structural transformation of porous polyoxometalate frameworks and highly efficient biomimetic aerobic oxidation of aliphatic alcohols, ACS Catal. 7 (2017) 6573–6580.

[33] J. Guo, Y. Niu, L. Song, Q. Xu, J. Lu, P. Ma, D. Zhang, C. Zhang, J. Niu, J. Wang, Synthesis, characterization and catalytic epoxidation properties of lanthanide-stabilized peroxoisopolytungstates, Dalton Trans. 46 (2017) 12981–12987.

[34] M. Sun, J. Zhang, P. Putaj, V. Caps, F. Lefebvre, J. Pelletier, J. Basset, Catalytic oxidation of light alkanes (C_1-C_4) by heteropoly compounds, Chem. Rev. 114 (2014) 981–1019.

[35] X. Han, C. Qin, X. Wang, Y. Tan, X. Zhao, E. Wang, Bio-inspired assembly of cubane-adjustable polyoxometalate-based high-nuclear nickel clusters for visible light-driven hydrogen evolution, Appl. Catal. B Environ. 211 (2017) 349–356.

[36] H. Li, S. Yao, H. Wu, J. Qu, Z. Zhang, T. Lu, W. Lin, E. Wang, Charge-regulated sequential adsorption of anionic catalysts and cationic photosensitizers into metal-organic frameworks enhances photocatalytic proton reduction, Appl. Catal. B Environ. 224 (2018) 46–52.

[37] H. Shi, Y. Yu, Y. Zhang, X. Feng, X. Zhao, H. Tan, S. Ullah Khan, Y. Li, E. Wang, Polyoxometalate/TiO_2/Ag composite nanofibers with enhanced photocatalytic performance under visible light, Appl. Catal. B Environ. 221 (2018) 280–289.

[38] D.J. Sures, S.A. Serapian, K. Kozma, P.I. Molina, C. Bob, M. Nyman, Electronic and relativistic contributions to ion-pairing in polyoxometalate model systems, Phys. Chem. Chem. Phys. 19 (2017) 8715–8725.

[39] C. Zhang, Y. Hong, R. Dai, X. Lin, L. Long, C. Wang, W. Lin, Highly active hydrogen evolution electrodes via co-deposition of platinum and polyoxometalates, ACS Appl. Mater. Interfaces 7 (2015) 11648–11653.

[40] S. Zhang, O. Oms, L. Hao, R. Liu, M. Wang, Y. Zhang, H. He, A. Dolbecq, J. Marrot, B. Keita, L. Zhi, P. Mialane, B. Li, G. Zhang, High oxygen reduction reaction performances of cathode materials combining polyoxometalates coordination complexes, and carboneous supports, ACS Appl. Mater. Interfaces 9 (2017) 38486–38498.

[41] W. Luo, J. Hu, H. Diao, B. Schwarz, C. Streb, Y. Song, Robust polyoxometalate/nickel foam composite electrodes for sustained electrochemical oxygen evolution at high pH, Angew. Chem. Int. Ed. 56 (2017) 4941–4944.

[42] S.S. Wang, G.Y. Yang, Recent advances in polyoxometalate-catalyzed reactions, Chem. Rev. 115 (2015) 4893–4962.

[43] J. Dong, J. Hu, Y. Chi, Z. Lin, B. Zou, S. Yang, C.L. Hill, C. Hu, A polyoxoniobate-polyoxovanadate double-anion catalyst for simultaneous oxidative and hydrolytic decontamination of chemical warfare agent simulants, Angew. Chem. Int. Ed. 56 (2017) 4473–4477.

[44] W. Guo, H. Lv, K.P. Sullivan, W.O. Gordon, A. Balboa, G.W. Wagner, D.G. Musaev, J. Bacsa, C.L. Hill, Broad-spectrum liquid- and gas-phase decontamination of chemical warfare agents by one-dimensional heteropolyniobates, Angew. Chem. Int. Ed. 55 (2016) 7403–7407.

[45] M.K. Kinnan, W.R. Creasy, L.B. Fullmer, H.L. Schreuder-Gibson, M. Nyman, Nerve agent degradation with polyoxoniobates: nerve agent degradation with polyoxoniobates, Eur. J. Inorg. Chem. 2014 (2014) 2361–2367.

[46] A. Yoshida, S. Hikichi, N. Mizuno, Acid–base catalyses by dimeric disilicoicosatungstates and divacant γ-Keggin-type silicodecatungstate parent: reactivity of the polyoxometalate compounds controlled by step-by-step protonation of lacunary WO sites, J. Organomet. Chem. 692 (2007) 455–459.

[47] K. Sugahara, T. Kimura, K. Kamata, K. Yamaguchi, N. Mizuno, A highly negatively charged c-Keggin germanodecatungstate efficient for Knoevenagel condensation, Chem. Commun. 48 (2012) 8422–8424.

[48] S. Zhao, Y. Chen, Y.F. Song, Tri-lacunary polyoxometalates of $Na_8H[PW_9O_{34}]$ as heterogeneous lewis base catalysts for knoevenagel condensation, cyanosilylation and the synthesis of benzoxazole derivatives, Appl. Catal. Gen. 475 (2014) 140–146.

[49] R. Khoshnavazi, L. Bahrami, F. Havasi, Organic–inorganic hybrid polyoxometalate and its graphene oxide–Fe3O4 nanocomposite, synthesis, characterization and their applications as nanocatalysts for the Knoevenagel condensation and the synthesis of 2,3-dihydroquinazolin-4(1H)-ones, RSC Adv. 6 (2016) 100962–100975.

[50] Y. Jia, Y. Fang, Y. Zhang, H.N. Miras, Y.F. Song, Classical keggin intercalated into layered double hydroxides: facile preparation and catalytic efficiency in knoevenagel condensation reactions, Chem. – Eur. J. 21 (2015) 14862–14870.

[51] S. Hayashi, S. Yamazoe, K. Koyasu, T. Tsukuda, Application of group V polyoxometalate as an efficient base catalyst: a case study of decaniobate clusters, RSC Adv. 6 (2016) 16239–16242.

[52] M. Nyman, Polyoxoniobate chemistry in the 21st century, Dalton Trans. 40 (2011) 8049–8058.

[53] W. Ge, X. Wang, L. Zhang, L. Du, Y. Zhou, J. Wang, Fully-occupied Keggin type polyoxometalate as solid base for catalyzing CO_2 cycloaddition and Knoevenagel condensation, Catal. Sci. Technol. 6 (2016) 460–467.

[54] Y.K. Hwang, D.Y. Hong, J.S. Chang, S.H. Jhung, Y.K. Seo, J. Kim, A. Vimont, M. Daturi, C. Serre, G. Ferey, Amine grafting on coordinatively unsaturated metal centers of MOFs: consequences for catalysis and metal encapsulation, Angew. Chem. 120 (2008) 4212–4216.

[55] W. Fan, Y. Wang, Z. Xiao, L. Zhang, Y. Gong, F. Dai, R. Wang, D. Sun, A stable amino-functionalized interpenetrated metal–organic framework exhibiting gas selectivity and pore-size-dependent catalytic performance, Inorg. Chem 56 (2017) 13634–13637.

[56] D.J. Macquarrie, D.B. Jackson, Aminopropylated MCMs as base catalysts: a comparison with aminopropylated silica, Chem. Commun. 0 (1997) 1781–1782.

[57] M. Trilla, R. Pleixats, M.W.C. Man, C. Bied, Organic-inorganic hybrid silica materials containing imidazolium and dihydroimidazolium salts as recyclable organocatalysts for Knoevenagel condensations, Green Chem. 11 (2009) 1815–1820.

[58] E. Gianotti, U. Diaz, S. Coluccia, A. Corma, Hybrid organic-inorganic catalytic mesoporous materials with proton sponges as building blocks, Phys. Chem. Chem. Phys. 13 (2011) 11702–11709.

[59] Z. Liang, J. Sun, D. Zhang, P. Ma, C. Zhang, J. Niu, J. Wang, Assembly of $TeO_3{}^{2-}$ ions embedded in an Nb/O cage with selective decolorization of organic dye, Inorg. Chem. 56 (2017) 10119–10122.

[60] A.D. Becke, A new mixing of Hartree–Fock and local density-functional theories, J. Chem. Phys. 98 (1993) 1372–1377.

[61] C. Lee, W. Yang, R.G. Parr, Development of the Colle-Salvetti correlation-energy formula into a functional of the electron density, Phys. Rev. B 37 (1988) 785–789.

[62] D. Feller, The role of databases in support of computational chemistry calculations, J. Comput. Chem. 17 (1996) 1571–1586.

[63] K.L. Schuchardt, B.T. Didier, T. Elsethagen, L. Sun, V. Gurumoorthi, J. Chase, J. Li, T.L. Windus, Basis set exchange: a community database for computational sciences, J. Chem. Inf. Model. 47 (2007) 1045–1052.